AMERICAN SOCIETY FOR MICROBIOLOGY | Journal of Bacteriology®

RESEARCH ARTICLE

Survival of Anaerobic Fe^{2+} Stress Requires the ClpXP Protease

Brittany D. Bennett,[a] Kaitlyn E. Redford,[a] Jeffrey A. Gralnick[a]

[a]BioTechnology Institute and Department of Plant and Microbial Biology, University of Minnesota—Twin Cities, St. Paul, Minnesota, USA

ABSTRACT *Shewanella oneidensis* strain MR-1 is a versatile bacterium capable of respiring extracellular, insoluble ferric oxide minerals under anaerobic conditions. The respiration of iron minerals results in the production of soluble ferrous ions, which at high concentrations are toxic to living organisms. It is not fully understood how Fe^{2+} is toxic to cells anaerobically, nor is it fully understood how *S. oneidensis* is able to resist high levels of Fe^{2+}. Here we describe the results of a transposon mutant screen and subsequent deletion of the genes *clpX* and *clpP* in *S. oneidensis*, which demonstrate that the protease ClpXP is required for anaerobic Fe^{2+} resistance. Many cellular processes are known to be regulated by ClpXP, including entry into stationary phase, envelope stress response, and turnover of stalled ribosomes. However, none of these processes appears to be responsible for mediating anaerobic Fe^{2+} resistance in *S. oneidensis*. Protein trapping studies were performed to identify ClpXP targets in *S. oneidensis* under Fe^{2+} stress, implicating a wide variety of protein targets. *Escherichia coli* strains lacking *clpX* or *clpP* also display increased sensitivity to Fe^{2+} anaerobically, indicating Fe^{2+} resistance may be a conserved role for the ClpXP protease system. Hypotheses regarding the potential role(s) of ClpXP during periods of high Fe^{2+} are discussed. We speculate that metal-containing proteins are misfolded under conditions of high Fe^{2+} and that the ClpXP protease system is necessary for their turnover.

IMPORTANCE Prior to the evolution of cyanobacteria and oxygenic photosynthesis, life arose and flourished in iron-rich oceans. Today, aqueous iron-rich environments are less common, constrained to low-pH conditions and anaerobic systems such as stratified lakes and seas, digestive tracts, subsurface environments, and sediments. The latter two ecosystems often favor dissimilatory metal reduction, a process that produces soluble Fe^{2+} from iron oxide minerals. Dissimilatory metal-reducing bacteria must therefore have mechanisms to tolerate anaerobic Fe^{2+} stress, and studying resistance in these organisms may help elucidate the basis of toxicity. *Shewanella oneidensis* is a model dissimilatory metal-reducing bacterium isolated from metal-rich sediments. Here we demonstrate a role for ClpXP, a protease system widely conserved in bacteria, in anaerobic Fe^{2+} resistance in both *S. oneidensis* and *Escherichia coli*.

KEYWORDS *Shewanella*, iron reduction, iron toxicity, proteases

The bacterium *Shewanella oneidensis* MR-1 is a member of the gammaproteobacteria that resides in the oxic-anoxic transition zones of water columns and aquatic sediments (1–3). *S. oneidensis* is a facultative anaerobe able to utilize numerous compounds as terminal electron acceptors in the absence of oxygen, including nitrate, sulfite, trimethylamine *N*-oxide, fumarate (1, 4, 5), and metals such as iron and manganese (hydr)oxide minerals (1, 6), which are frequently abundant in aquatic sediments (7). The respiration and consequent change in oxidation state of a metal can influence its solubility. For example, ferric iron (Fe^{3+}) is often found in sediments as insoluble iron

Received 6 November 2017 **Accepted** 23 January 2018

Accepted manuscript posted online 29 January 2018

Citation Bennett BD, Redford KE, Gralnick JA. 2018. Survival of anaerobic Fe^{2+} stress requires the ClpXP protease. J Bacteriol 200:e00671-17. https://doi.org/10.1128/JB.00671-17.

Editor George O'Toole, Geisel School of Medicine at Dartmouth

Address correspondence to Jeffrey A. Gralnick, gralnick@umn.edu.

oxides (8), but upon reduction, these minerals can dissolve and release soluble ferrous iron (Fe^{2+}) (8, 9).

Like many transition metals, iron is required for numerous biological functions (10), but at higher concentrations, it becomes toxic to organisms (11–13). Fe^{2+} toxicity in aerobic conditions is believed to be due to oxidative stress resulting from the production of hydroxyl radicals (12, 14, 15), but the mechanism of anaerobic Fe^{2+} toxicity is not known. *S. oneidensis* is capable of tolerating millimolar levels of Fe^{2+} anaerobically (6), higher than many other bacterial species (13, 16, 17), consistent with an adaptation to metal-rich environments. *S. oneidensis* is able to limit the buildup of intracellular iron via the activities of the iron uptake regulator Fur, which suppresses the production of siderophores and iron import systems under iron-replete conditions (18–20). The inner membrane efflux protein FeoE removes excess Fe^{2+} from the cytoplasm produced during Fe^{3+} respiration and lowers Fe^{2+} sensitivity (21). To discover other Fe^{2+} resistance mechanisms encoded in the *S. oneidensis* genome and to uncover mechanisms of anoxic Fe^{2+} toxicity, we performed a transposon screen under excess-Fe^{2+} conditions. Here we present analysis of two genes that, upon inactivation, conferred a fitness defect in the presence of excess Fe^{2+}: *clpP* and *clpX*.

clpP and *clpX* encode the AAA+ (ATPases associated with diverse cellular activities) cytoplasmic protease ClpXP. The ATP-dependent unfoldase ClpX recognizes substrate proteins (22) and feeds them into the serine protease ClpP, which degrades the unfolded target proteins into small peptides (23, 24). ClpA, a second unfoldase able to complex with ClpP in place of ClpX (24), targets a different but overlapping set of proteins for degradation by ClpP in *Escherichia coli* (22, 25). ClpXP is one of five AAA+ proteases encoded in the *S. oneidensis* genome, the other four being ClpAP, Lon, HslVU, and FtsH (26–30). ClpXP has several established roles in bacteria, including regulation of entry into stationary phase via degradation of the stress response regulator σ^S, degradation of cell division proteins, promoting release of the envelope stress response regulator σ^E, and turning over ribosomes by degrading proteins stalled during translation (25, 31–36). We demonstrate that the role of ClpXP in mediating resistance to anaerobic Fe^{2+} stress is independent of these previously established roles. A role for ClpXP in Fe^{2+} tolerance may extend beyond *S. oneidensis*, as *clpPX* genes from *E. coli* complement the Fe^{2+} toxicity phenotype of *S. oneidensis clpPX* mutants and *E. coli* strains defective in either *clpX* or *clpP* exhibit enhanced sensitivity to Fe^{2+} under anaerobic conditions.

RESULTS

Tn-Seq reveals genes required for anaerobic Fe^{2+} toxicity response. To find genes involved in surviving high concentrations of Fe^{2+} anaerobically, transposon sequencing (Tn-Seq) was performed on wild-type and Δ*feoE* mutant *S. oneidensis* libraries grown in the presence or absence of 0.8 mM $FeCl_2$. Both wild-type and Δ*feoE* strains were used in order to serve as replicates for the experiment while providing a means to discover genes that, upon deactivation, confer a stronger fitness defect in a strain with increased Fe^{2+} sensitivity (Δ*feoE* mutant) (21). The results of the Tn-Seq screen are listed in Table S1 in the supplemental material. The fitness costs of genes required for anaerobic respiration or encoding proteins known to interact with Fe^{2+} were evaluated as controls to confirm the validity of the Tn-Seq results. Deactivation of genes encoding the fumarate reductase FccA, pyruvate formate-lyase PflB, and inner membrane tetraheme cytochrome CymA conferred strong defects for each strain under both outgrowth conditions (Table S1; see Materials and Methods for an explanation of fitness effect calculations), confirming that the Tn-Seq screen reflects genes required for growth under our conditions. Deactivation of *feoE*, which encodes an Fe^{2+} efflux pump (21), conferred a significant net fitness defect under high Fe^{2+} (−1.24) (Table S1) in the wild-type background. No reads were mapped to *feoE* in any of the Δ*feoE* libraries, indicating that no cross-library contamination had occurred. Deactivation of *feoB*, which encodes an Fe^{2+} importer in *E. coli* (37), conferred a strong apparent net fitness benefit under high-Fe^{2+} conditions in both the wild-type and Δ*feoE* mutant (+3.68 and +1.77,

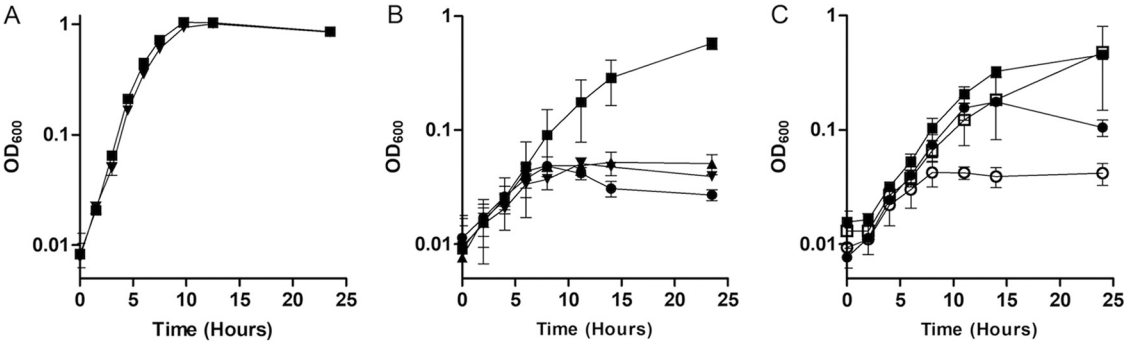

FIG 1 Growth of Δ*clpP*, Δ*clpX*, and Δ*clpPX* mutants with and without high $FeCl_2$. (A) The rate of growth in anoxic LB supplemented with 20 mM lactate and 40 mM fumarate was measured for wild-type *S. oneidensis* (■) and the Δ*clpPX* mutant (▼). (B) The rate of growth in anoxic LB supplemented with 20 mM lactate, 40 mM fumarate, and 2 mM $FeCl_2$ was measured for wild-type *S. oneidensis* (■) and the Δ*clpPX* (▼), Δ*clpX* (▲), and Δ*clpP* (●) mutants. (C) The rate of growth in anoxic LB supplemented with 20 mM lactate, 40 mM fumarate, and 2 mM $FeCl_2$ was measured for wild-type *S. oneidensis* with empty pBBR1MCS-2 (□), wild-type *S. oneidensis* with pBBR1MCS-2::*clpPX* (■), the Δ*clpPX* mutant with empty pBBR1MCS-2 (○), and the Δ*clpPX* mutant with pBBR1MCS-2::*clpPX* (●). Results are the mean ± 1 standard deviation from three biological replicates.

respectively) (Table S1). Under low-Fe^{2+} conditions, *feoB* mutations result in a strong fitness defect, which is partially rescued in the Δ*feoE* background (−4.00 in the wild type and −2.54 in the Δ*feoE* mutant) (Table S1), consistent with their opposing functions.

Two genes that, upon deactivation, produced some of the strongest net fitness defects under high Fe^{2+} were *clpP* (SO_1794) and *clpX* (SO_1795) (−1.09 and −1.55 in the wild-type background and −2.05 and −2.73 in the Δ*feoE* mutant, respectively) (Table S1). Of the genes encoding the five AAA+ proteases in the *S. oneidensis* genome, only deactivation of *clpX* and *clpP* conferred a significant defect in the presence of excess Fe^{2+} in our transposon mutant screen. To confirm the Tn-Seq results for *clpP* and *clpX*, in-frame single and double deletions were made of *clpP* and *clpX* from the *S. oneidensis* genome. The Δ*clpP*, Δ*clpX*, and Δ*clpPX* mutants had strong growth defects compared to the wild type when grown anaerobically in LB supplemented with 20 mM lactate, 40 mM fumarate, and 2 mM $FeCl_2$ but not when $FeCl_2$ was omitted (doubling times without added Fe^{2+}: Δ*clpPX* mutant, 1.23 ± 0.14 h; wild type, 1.22 ± 0.11 h) (Fig. 1A and B). Complementation with pBBR1MCS-2::*clpPX* restored the growth rate of the Δ*clpPX* mutant to that of the wild type (Fig. 1C).

ClpXP role in anaerobic Fe^{2+} resistance is unrelated to known proteolytic functions. Much of the research into the function and structure of ClpXP has taken place in *E. coli*, although as mitochondria and additional bacterial species are analyzed, the known roles of ClpXP are expanding (reviewed in references 38 to 40). We focused the investigation of known ClpXP proteolysis targets to those annotated in the *S. oneidensis* genome. ClpXP targets the starvation and stationary-phase regulator sigma factor σ^S (31) and degrades proteins stalled in translation via recruitment and recognition by SspB, SmpB, and the SsrA transfer-mRNA tag (35, 41, 42). None of the fitness costs of deactivating any of these genes during growth in high Fe^{2+} met our threshold for significance in the Tn-Seq data set (*rpoS*, −0.08; *sspB*, −0.57; *ssrA*, +0.19; and *smpB*, +0.36 in the wild-type background; −0.77, −0.86, −0.53, and −1.65, respectively, in the Δ*feoE* mutant) (Table S1). While *smpB* appears to have a significant result in the Δ*feoE* background, the number of reads that mapped to *smpB* in the Δ*feoE* background was low (50% less than the standard cutoff [Table S1]) and may therefore be an unreliable estimate of fitness.

A group of *E. coli* proteins regulated by ClpXP are the cell division proteins FtsZ, ZapC, FtsA, MinD, and SulA (25, 32, 33). Deactivation of neither *zapA*, *zapB*, *zapC*, *ftsA*, *minD*, nor *sulA* conferred a significant net fitness defect in high Fe^{2+} in our Tn-Seq data (−0.34, +0.33, +0.47, +0.85, −0.15, and +0.29, respectively, in the wild-type background; −0.57, −0.41, +0.53, −0.52, −0.22, and +0.35, respectively, in the Δ*feoE*

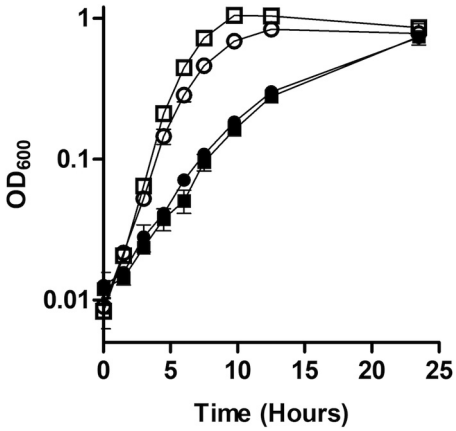

FIG 2 Growth of the Δ*rpoE* mutant with high $FeCl_2$. The rate of growth in anoxic LB supplemented with 20 mM lactate and 40 mM fumarate, with (closed symbols) or without (open symbols) 2.5 mM $FeCl_2$, was measured for wild-type *S. oneidensis* (□ and ■) and the Δ*rpoE* mutant (○ and ●). Results are the mean ± 1 standard deviation from three biological replicates.

mutant) (Table S1). *ftsZ* appears to be an essential gene in *S. oneidensis* according to our Tn-Seq data, as no sequencing reads were mapped to the gene in any of the libraries (Table S1), consistent with previous observations (43).

ClpXP is involved in the release of the stress response sigma factor σ^E by degrading the cytoplasmic domain of the anti-sigma factor RseA (34). The proteases DegS and RseP are also required for degradation of RseA (44, 45), while RseB acts as a secondary regulator of σ^E (46). None of the genes encoding proteins involved in regulating σ^E had significant net fitness costs upon deactivation under high Fe^{2+} in our Tn-Seq data (+0.61, −0.42, +0.09, and +0.31 in the wild-type background, respectively; +0.41, −0.80, −0.65, and +0.64, respectively, in the Δ*feoE* mutant) (Table S1). However, deactivation of *rpoE* itself, the gene encoding σ^E, did confer a net fitness defect near our significance threshold in high Fe^{2+} (−0.92 in the wild-type background, −1.06 in the Δ*feoE* mutant). However, an in-frame *rpoE* deletion mutant was not significantly impaired compared to the wild type in either the presence or absence of excess Fe^{2+} (doubling times, respectively, of 3.13 ± 0.21 and 2.94 ± 0.21 h in excess Fe^{2+} and 1.38 ± 0.20 and 1.22 ± 0.11 h without excess Fe^{2+}) (Fig. 2). Together, these data suggest that ClpXP plays a role in promoting survival during anaerobic Fe^{2+} stress, but this role is not related to previously described functions of ClpXP.

ClpXP targets a distinct subset of proteins under high-Fe^{2+} conditions. To determine the proteolysis targets of ClpXP under high-Fe^{2+} conditions, we set up a ClpP trapping experiment modified from that of Flynn et al. (25). The catalytic serine in the active site of ClpP was mutated (S106A) to eliminate proteolytic activity, and a His_6-TEV-Myc_3 affinity tag was attached to the C terminus, creating $ClpP^{Trap}$. An allele encoding a protein without a mutated active site (S106) was also created, called $ClpP^{Tag}$, to confirm activity of the tagged protein. $ClpP^{Trap}$ folds correctly and continues to bind the ATPase subunits ClpA and ClpX (25), which feed protease targets into $ClpP^{Trap}$. Substrate proteins are slowly released by $ClpXP^{Trap}$ or $ClpAP^{Trap}$ (47), allowing for the use of $ClpP^{Trap}$, in conjunction with protein mass spectrometry, to detect which proteins are targeted for degradation by ClpXP or ClpAP.

A Δ*smpB* Δ*clpP* background was used for all trapping strains, in order to remove SsrA-tagged proteins from protein analysis and to prevent degradation of ClpXP targets by an active ClpP protease (25). *clpA* and *clpX* deletions were created in this background to isolate proteins specifically targeted for degradation by either ClpXP or ClpAP. Additionally, a Δ*clpA* Δ*clpX* mutant was used to identify proteins that nonspecifically bind to $ClpP^{Trap}$ or the anti-Myc resin without being targeted by ClpX or ClpA. Each strain was transformed with pBBR1MCS-2::$clpP^{Trap}$.

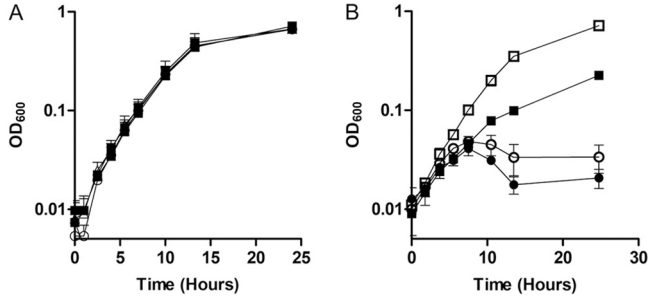

FIG 3 Growth of proteomic analysis strains. (A) The rate of growth in anoxic LB supplemented with 20 mM lactate, 40 mM fumarate, and 2 mM $FeCl_2$ was measured for wild-type *S. oneidensis* (■) and the Δ*smpB* (○) and Δ*clpA* (Δ) mutants. (B) The rate of growth in anoxic LB supplemented with 20 mM lactate, 40 mM fumarate, and 2.5 mM $FeCl_2$ was measured for wild-type *S. oneidensis* with empty pBBR1MCS-2 (□), the Δ*smpB* Δ*clpA* Δ*clpP* mutant with empty pBBR1MCS-2 (○), the Δ*smpB* Δ*clpA* Δ*clpP* mutant with pBBR1MCS-2::$clpP^{Tag}$ (■), and the Δ*smpB* Δ*clpA* Δ*clpP* mutant with pBBR1MCS-2::$clpP^{Trap}$ (●). Results are the mean ± 1 standard deviation from three biological replicates.

To confirm that deletion of *smpB* and *clpA* did not affect the growth of *S. oneidensis* under high-Fe^{2+} conditions, the wild-type and Δ*smpB* and Δ*clpA* mutants were grown anaerobically in LB supplemented with 20 mM lactate, 40 mM fumarate, and 2 mM $FeCl_2$. There was no difference in growth rates between the wild type and Δ*smpB* and Δ*clpA* mutants (doubling times of 2.36 ± 0.22, 2.34 ± 0.35, and 2.52 ± 0.35 h, respectively) (Fig. 3A). The Δ*smpB* Δ*clpP* Δ*clpA* mutant with pBBR1MCS-2::$clpP^{Trap}$ had the same growth defect as the Δ*smpB* Δ*clpP* Δ*clpA* mutant with empty pBBR1MCS-2 when grown in anaerobic LB supplemented with 20 mM lactate, 40 mM fumarate, and 2 mM $FeCl_2$ (Fig. 3B), confirming that the S106A mutation mimics the phenotype of a *clpP* null mutant. The Δ*smpB* Δ*clpP* Δ*clpA* mutant with pBBR1MCS-2::$clpP^{Tag}$ had a higher growth rate than the Δ*smpB* Δ*clpP* Δ*clpA* mutant with pBBR1MCS-2::$clpP^{Trap}$ (Fig. 3B), suggesting that removal of the propeptide sequence from and addition of the purification tag to ClpP did not interfere with its proper folding.

The three ClpP-trapping strains were grown anaerobically in LB supplemented with 20 mM lactate and fumarate; the ClpX-only strain was also grown in anaerobic LB supplemented with 20 mM lactate, 40 mM fumarate, and 1.1 mM $FeCl_2$. ClpP-trapped proteins were identified using mass spectrometry. The proteins listed in Table 1 were detected at least twice as frequently in the Fe^{2+} culture as in any of the others in at least two of three mass spectrometry runs. Proteins trapped by ClpXP that were enriched under high-Fe^{2+} conditions have disparate functions but frequently (10 of 11 proteins trapped) contain metal binding sites (Table 1; see Table S3 in the supplemental material), a higher proportion than the proteins trapped with ClpXP under lower-Fe^{2+} conditions (12 of 19), ClpAP (1 of 3), either ClpAP or ClpXP (17 of 36), or ClpP with no ATPase adapter (1 of 2). Additionally, a higher proportion of proteins (7 of 11 [Table 1; Table S3]) trapped with ClpXP in high Fe^{2+} utilize nucleotide-derived cofactors than those trapped by ClpXP under lower Fe^{2+} (8 of 19).

Mg^{2+} concentration affects the growth of *S. oneidensis* in high Fe^{2+}. The protein trapping results indicated that a high intracellular ratio of Fe^{2+} to other metals might interfere with proper insertion of noniron metals into metalloproteins. To determine the effect of low Mg^{2+} concentration during growth in high Fe^{2+}, wild-type *S. oneidensis* was grown in *Shewanella* basal medium (SBM) with either 475 or 119 μM $MgSO_4$ (100% and 25% of the $MgSO_4$ concentrations in SBM, respectively) and with or without 0.8 mM $FeCl_2$. The lower concentration of Mg^{2+} did not affect the growth rate of *S. oneidensis* in the absence of Fe^{2+}; however, the growth rate was lower in the combination of high Fe^{+} and low Mg^{2+} than in high Fe^{2+} alone (Fig. 4).

ClpXP is required for Fe^{2+} resistance in *E. coli*. To determine whether ClpXP is involved in Fe^{2+} resistance beyond *S. oneidensis*, we grew *S. oneidensis* Δ*clpX* and Δ*clpP* mutants complemented with *E. coli clpX* and *clpP* genes, respectively, in anaerobic LB supplemented with 20 mM lactate, 40 mM fumarate, and 2.5 mM $FeCl_2$. The *clpX* and

TABLE 1 Proteins differentially trapped by ClpXP in high or low Fe^{2+}

Protein	Locus	Predicted function	Predicted features(s) or ligand(s)[a]
Trapped in high Fe^{2+}			
RecA	SO_3430	Recombinase A	ATP, Mg^{2+}
DeaD	SO_4034	ATP-dependent RNA helicase	DEAD, ATP, Mg^{2+}
NrdA	SO_2415	Aerobic ribonucleoside-diphosphate reductase alpha subunit	Tyrosyl radical, rNTP, ATP, Fe^{3+}
NrdD	SO_2834	Anaerobic ribonucleoside-triphosphate reductase	Glycyl radical, rNTP, ATP, Zn^{2+}
GapA	SO_2345	Glyceraldehyde-3-phosphate dehydrogenase	G3P, NAD(P)
TnpB_MuSo2	SO_2655	Mu phage transposase OrfB	ATPase, DNA, ATP, Mg^{2+}
CydA	SO_3286	Cytochrome *d* ubiquinol oxidase subunit I	TM, UQ, heme
MgtE-1	SO_1145	Divalent metal transporter	TM, CBS, MgtE-N, Mg^{2+}, Ca^{2+}
	SO_0520	Heavy metal efflux pump permease component CzcA family	TM, Cu^{2+}
	SO_1383	ATP-dependent RNA helicase DEAD box family	DEAD, ATP, Mg^{2+}
LepB	SO_1347	Signal peptidase I	TM, S26, Mg^{2+}, K^{+}
Trapped in low Fe^{2+}			
AtpA	SO_4749	ATP synthase subunit alpha	Mg^{2+}, ADP, ATP
SecA	SO_4211	Protein translocase subunit	Zn^{2+}, ATP
ThrS	SO_2299	Threonine-tRNA ligase	Zn^{2+}, ATP, Thr, anticodon binding
GlyS	SO_0014	Glycine-tRNA ligase beta subunit	ATP, Gly, anticodon binding
Fba	SO_0933	Fructose-bisphosphate aldolase class II	Zn^{2+}, Na^{+}, DAP
	SO_3743	Transcriptional regulator TetR family	HTH
DmsA	SO_1429	Extracellular dimethyl sulfoxide/manganese oxide reductase molybdopterin-binding subunit A	Fe-S, MopB
AdhB	SO_1490	Alcohol dehydrogenase II	Fe^{3+}
	SO_0988	Molybdopterin-binding oxidoreductase	Fe-S, Mo^{5+}
DeoD2	SO_1221	Purine nucleoside phosphorylase DeoD-type 2	Purine nucleoside, phosphate
ZapC	SO_2591	Cell division protein	Z-ring binding
Ppc	SO_0274	Phosphoenolpyruvate carboxylase	Mg^{2+}
HemB	SO_2587	Delta-aminolevulinic acid dehydratase	Zn^{2+}, Mg^{2+}, Schiff base
	SO_3363	Transcriptional regulator LysR family	PBP, HTH
NuoG	SO_1016	NADH-quinone oxidoreductase subunit G	Fe-S, NADH, UQ
	SO_1117	Cytoplasmic leucyl metal-dependent aminopeptidase	Zn^{2+}/Mn^{2+}
NadB	SO_1341	L-Aspartate oxidase	FAD, SQO
FdhD	SO_0107	Sulfurtransferase	Mo-*bis*PGD
	SO_3097	Anti-sigma factor	TM; DUF3379

[a]DEAD, DEAD box RNA helicase domain; TM, transmembrane domain; UQ, ubiquinone binding domain; CBS, cystathionine beta-synthase-like ligand binding domain; MgtE-N, Mg^{2+} transporter intracellular N domain; S26, S26 signal peptidase domain; DAP, dihydroxyacetone phosphate; HTH, helix-turn-helix DNA binding domain; Fe-S, iron-sulfur cluster; MopB, molybdopterin-binding domain; PBP, periplasmic effector binding pocket; FAD, flavin adenine dinucleotide; SQO, succinate:quinone oxidoreductase domain; Mo-*bis*PGD, molybdo-*bis* pyranopterin guanine dinucleotide.

clpP genes from *E. coli* complemented the Fe^{2+} sensitivity phenotype of Δ*clpX* and Δ*clpP S. oneidensis* strains (Fig. 5A). *E. coli* strains with deletions of either *clpX* or *clpP* were grown in anaerobic LB supplemented with 20 mM lactate and 40 mM fumarate, with or without 6 mM $FeCl_2$. This Fe^{2+} concentration was required to see impairment in the growth rate of *E. coli* in LB. While the Δ*clpX* and Δ*clpP* mutants grew at the same rate as the wild type without added Fe^{2+}, both strains displayed a growth defect in the presence of excess Fe^{2+} (Fig. 5B).

DISCUSSION

AAA+ proteases have been implicated in numerous cellular processes in various bacterial species. Here we have provided evidence for a new function of the AAA+ protease ClpXP: resistance to Fe^{2+} toxicity. The loss of either *clpP* or *clpX* was shown to be detrimental to both *S. oneidensis* and *E. coli* growing under high-Fe^{2+} conditions but not at low Fe^{2+} concentrations (Fig. 1B and 5B; see Table S1 in the supplemental material). The loss of *clpA*, which encodes another ATP-dependent chaperone that complexes with ClpP (24), or *clpS*, which encodes an adaptor to the ClpAP complex (48), had no effect on the sensitivity of *S. oneidensis* to high Fe^{2+} concentrations (Fig. 3A; Table S1), indicating that the proteins specifically targeted by ClpX but not ClpA for degradation by ClpP are involved in Fe^{2+} sensitivity.

ClpXP regulates a number of cytoplasmic proteins and facilitates the turnover of stalled ribosomes (25, 31–34). None of these processes, however, appears to be

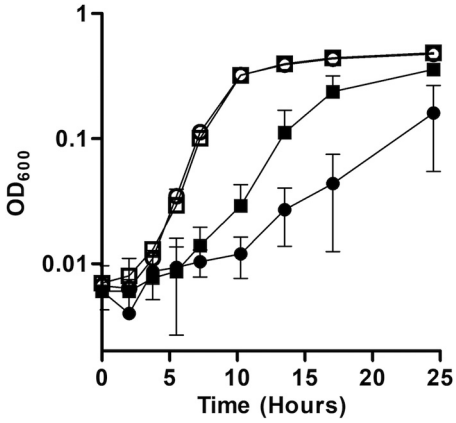

FIG 4 Growth of *S. oneidensis* with high Fe^{2+} and low Mg^{2+}. The rate of growth in anoxic SBM supplemented with 20 mM lactate, 40 mM fumarate, and 475 μM $MgSO_4$ and 0 mM $FeCl_2$ (□), 119 μM $MgSO_4$ and 0 mM $FeCl_2$ (○), 475 μM $MgSO_4$ and 0.8 mM $FeCl_2$ (■), or 119 μM $MgSO_4$ and 0.8 mM $FeCl_2$ (●) was measured for wild-type *S. oneidensis*. Results are the mean ± 1 standard deviation from three biological replicates.

involved in the resistance of *S. oneidensis* to high Fe^{2+} concentrations (Fig. 2 and 3; Table S1). Previous studies of σ^E in *E. coli* have indicated that *rpoE* is essential and that mutants can be made only in conjunction with suppressor mutations (49). Suppressor mutations could explain why we did not see an increase in Fe^{2+} sensitivity for our Δ*rpoE* strain; however, we believe that σ^E is neither essential in *S. oneidensis* nor critical for Fe^{2+} stress response. *rpoE* transposon and deletion mutants were readily generated (Fig. 2; Table S1), inconsistent with the requirement of a suppressor mutation. Additionally, we tested multiple Δ*rpoE* isolates, all of which displayed identical phenotypes regarding resistance to Fe^{2+} and sensitivity to other stressors (data not shown). Therefore, the role ClpXP plays in Fe^{2+} resistance does not appear to be mediated through the promotion of σ^E release or other previously described ClpXP targets.

As we could not identify the function of ClpXP in response to Fe^{2+} toxicity through Tn-Seq data or phenotypic tests with deletion mutants, we adapted a ClpP trapping method (25) to identify ClpXP proteolysis targets in *S. oneidensis*. While one-fourth to one-third of cellular proteins are believed to require a metal cofactor (81), nearly all proteins that were enriched for ClpXP trapping under high-Fe^{2+} conditions are predicted to contain metal-binding domains (91% [Table 1]), more than for the proteins trapped by ClpXP in lower Fe^{2+} (57% [Table 1; Table S3]). Additionally, 64% of the

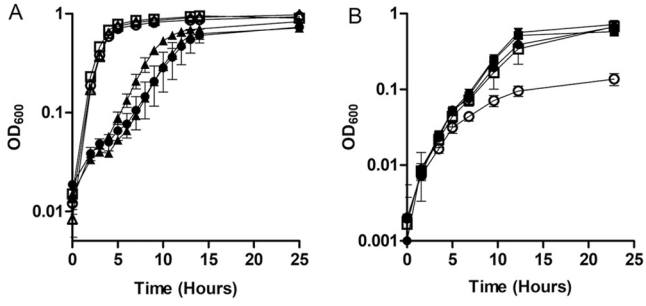

FIG 5 Growth of *E. coli* and *S. oneidensis* Δ*clpX* and Δ*clpP* mutant strains with and without high $FeCl_2$. (A) The rate of growth in anoxic LB supplemented with 20 mM lactate, 40 mM fumarate, and with (closed symbols) or without (open symbols) 6 mM $FeCl_2$ was measured for wild-type *E. coli* (□ and ■), the Δ*clpX* mutant (△ and ▲), and the Δ*clpP* mutant (○ and ●). (B) The rate of growth in anoxic LB supplemented with 20 mM lactate, 40 mM fumarate, and 2.5 mM $FeCl_2$ was measured for wild-type *S. oneidensis* with empty pBBR1MCS-2 (□), the Δ*clpPX* mutant with empty pBBR1MCS-2 (○), the Δ*clpPX* mutant with pBBR1MCS-2::$clpPX_{MR-1}$ (■), the Δ*clpPX* mutant with pBBR1MCS-2::$clpPX_{E.\ coli}$ (▼), and the Δ*clpX* mutant with pBBR1MCS-2::$clpX_{E.\ coli}$ (●). Results are the mean ± 1 standard deviation from three biological replicates.

proteins enriched for trapping by ClpXP under high Fe^{2+} are predicted to utilize nucleotides or nucleotide derivatives as cofactors, a higher proportion than with proteins enriched for ClpXP trapping under lower Fe^{2+} (42% [Table 1; Table S3]). The mass spectrometry data provided here are meant to be qualitative and can be only suggestive of relative quantitation; truly quantitative measurements would need to be performed in future studies. That said, the protein trapping results were largely repeatable. Given the controls and conditions used here, the proteomics results suggest to us the hypothesis that ClpXP may target metalloproteins and/or proteins with nucleotide-derived cofactors in *S. oneidensis* under Fe^{2+} stress.

Fe^{2+} has an affinity for pyrophosphate and nucleotides (51, 52), where it is predicted that Fe^{2+} complexes with phosphate ester oxygens (52). It may be that free Fe^{2+} binds to the phosphate groups of nucleotide cofactors in proteins, perhaps forcing a change in conformation around the cofactor. Alternatively, high soluble Fe^{2+} may cause inappropriate phosphate hydrolysis and interfere with enzymatic function.

In addition to binding nucleotides, iron and other metals bind readily to hydrophilic regions within proteins (53). It is notable that many proteins apparently targeted by $ClpP^{Trap}$ under the high-Fe^{2+} condition bind Mg^{2+} (Table 1; Table S3). The Irving-Williams series places the order of metal affinity to proteins as $Ca^{2+} < Mg^{2+} < Mn^{2+} < Fe^{2+} < Co^{2+} < Ni^{2+} < Cu^{2+} > Zn^{2+}$ (54), making Fe^{2+} likelier to bind proteins than Mg^{2+}, Ca^{2+}, Mn^{2+}, and, under certain conditions, Zn^{2+}. Cells have delivery systems to direct the insertion of most metals into their proper protein binding sites (50, 55–61). Proper insertion of metals at the lower end of the Irving-Williams series, such as Mn^{2+} and Mg^{2+}, on the other hand, frequently simply depends upon high relative intracellular concentrations of those metals (62, 63).

The intracellular concentration of Mg^{2+} is commonly kept around 1 mM, the highest concentration of all metals that have been evaluated (64). Not coincidentally, the intracellular concentration of each metal in the Irving-Williams series is inversely correlated with its affinity for proteins (64), indicating that cells compensate for low binding affinity with high relative concentration. It is therefore not surprising that Mg^{2+}-binding proteins appeared to be more frequently targeted by ClpXP under high Fe^{2+} in our study: as the concentration of Fe^{2+} rises, it may overwhelm the cells' iron storage and/or trafficking capacity and begin outcompeting Mg^{2+} and other metals less dependent on specific delivery systems for insertion into the correct protein binding sites.

Consistent with the hypothesis that high Fe^{2+} concentrations interfere with Mg^{2+} insertion into metalloproteins, lowering the Mg^{2+} concentration in the presence of high Fe^{2+} further decreased the growth rate of *S. oneidensis* beyond that in high Fe^{2+} alone (Fig. 4). Additionally, inactivation of the *corA* gene in our Tn-Seq screen caused a strong net fitness defect in both the wild type and Δ*feoE* mutant under high Fe^{2+} (-1.23 and -1.70, respectively) (Table S1). The stronger defect in the Δ*feoE* mutant indicates that the higher intracellular Fe^{2+} concentration in this mutant exacerbates the effect of *corA* mutation. CorA has a high affinity for Mg^{2+} (65, 66) and appears to be the primary Mg^{2+} importer in bacteria (67). Further lowering the ratio of Mg^{2+} to Fe^{2+} appears to increase sensitivity to Fe^{2+}, which could be due to mismetallation of Mg^{2+}-requiring proteins. Based on these results, we suggest that protein mismetallation may be at least one mechanism of Fe^{2+} toxicity to cells.

While Fe^{2+} is known to be toxic under aerobic conditions due to Fenton chemistry and the production of reactive oxygen species (12, 14, 15), the mechanism by which Fe^{2+} is toxic under anaerobic conditions has not been well understood. Previously published hypotheses about anoxic Fe^{2+} toxicity have included formation of organic radicals, inhibition of the F-ATPase (13), or reduction of Cu^{2+} to the more toxic Cu^{+} (68). Based on our findings in this study, we propose that mechanisms by which Fe^{2+} may be toxic anaerobically may include either binding nucleotide-derived cofactors or, as we believe to be more likely, overwhelming the normal mechanisms of proper metal insertion into metalloproteins, with Fe^{2+} replacing the required metal. Either of these events would interfere with proper enzyme activity, causing a buildup of multiple

inactive cytoplasmic proteins that could overwhelm the cell if not properly turned over. This hypothesis is consistent with the growth behavior of the strains lacking ClpX, ClpP, and ClpXP, where the growth rate is identical to that of the wild type for the first ~6 h before plateauing and beginning to decline (Fig. 1B). The growth pattern here is similar to that for temperature-sensitive mutations in the major chaperonin GroEL, which causes the accumulation of unfolded proteins (69). Interestingly, there was less overlap between our list of ClpXP-trapped proteins and those identified by Flynn et al. (25) than we expected. It may be that Fe^{2+} stress upends the usual set of ClpXP targets by making a certain subset of proteins more likely to become unstable or to partially unfold. If mismetallation of metalloproteins is a major mechanism behind Fe^{2+} toxicity, it is likely to be a major toxicity mechanism for other metals higher on the Irving-Williams series. In this case, ClpXP could target proteins with any misincorporated metal for degradation.

Here we have determined that ClpXP is an important factor in anaerobic Fe^{2+} resistance in both *E. coli* and *S. oneidensis*. Many bacterial species occasionally encounter high concentrations of metals, and consequently they have developed cellular mechanisms of metal toxicity resistance. *S. oneidensis*, for example, requires several mechanisms to resist the high Fe^{2+} concentrations that occur transiently and locally during the respiration of iron minerals. While the mechanism of ClpXP in resisting high Fe^{2+} needs to be confirmed with future work, the work presented here is consistent with our proposed model in which ClpXP is required to turn over misfolded proteins when cells experience anaerobic Fe^{2+} stress.

MATERIALS AND METHODS

Bacterial strains and growth conditions. Table 2 lists the bacterial strains and plasmids used in this work. The chemicals used throughout were the highest purity available through Sigma-Aldrich, unless otherwise indicated. *S. oneidensis* MR-1 was isolated from Lake Oneida, NY (1). The *E. coli* strains for cloning (UQ950) and mating (WM3064) are described by Saltikov et al. (70). Overnight liquid Luria-Bertani (LB; BD Difco) cultures, supplemented with 50 μg/ml kanamycin when appropriate, were inoculated with isolated colonies from freshly streaked −80°C stocks. *S. oneidensis* and *E. coli* cultures were grown at 30 and 37°C, respectively. Cultures were grown in LB or *Shewanella* basal medium (SBM [71]) supplemented with 5 ml/liter vitamin solution (72), 5 ml/liter trace mineral solution (73), and 0.05% (wt/vol) Casamino Acids. Anaerobic cultures were sealed with butyl rubber stoppers, flushed with nitrogen gas, and supplemented with 20 mM sodium lactate and 40 mM sodium fumarate. Liquid cultures, except for 1-liter cultures prepared for protein purification, were shaken at 250 rpm.

Creation and analysis of Tn-Seq mutant libraries. Transposon library creation and selection were performed as previously described (43). Briefly, a delivery vector with MmeI restriction sites surrounding the MiniHimar transposon, which randomly inserts into the chromosome at TA sites (74), was transferred into wild-type and Δ*feoE* mutant *S. oneidensis* strains via conjugation. Parent transposon libraries were outgrown for selection in anaerobic SBM with or without 0.8 mM $FeCl_2$. The concentration of 0.8 mM $FeCl_2$ was chosen to allow for an overall doubling time relatively close to that of unamended cultures while still inhibiting growth of Fe^{2+}-sensitive mutants. Cultures were harvested and DNA extracted after approximately five doublings. Parent and outgrown DNA libraries were processed and sequenced as previously described (75). Adapters and primers used to prepare the DNA for sequencing have been published previously (76). Briefly, DNA was phenol-chloroform extracted and digested with MmeI. Adapters containing library-identifying barcodes were ligated to the digested DNA, and the transposon insertion sites were PCR amplified using primers containing Illumina-specific sequences. Single-read 50-bp sequence analysis was performed on an Illumina HiSeq250 at the University of Minnesota Genomics Center. Downstream sequence processing was performed using the Galaxy server maintained by the Minnesota Supercomputing Institute. Between 20 million and 33 million reads were mapped to the *S. oneidensis* chromosome and megaplasmid (accession no. NC_004347.2 and NC_004349.1, respectively) for each parent and outgrown library. Reads that did not match the genome sequence 100%, did not match uniquely to a gene, or fell in the first 1% or last 10% of a coding sequence were omitted from analysis. The number of reads for each gene was normalized to the total number of reads in each library.

Fitness effects of each gene under the outgrowth conditions were calculated by taking the natural log of the normalized number of reads in the outgrowth libraries divided by that in the parent library. Tn-Seq calculations and results are reported in Table S1 in the supplemental material. To exclude genes that confer a growth benefit or defect upon deactivation regardless of Fe^{2+} concentration, the net fitness effect of growing in excess Fe^{2+} for each gene was calculated by subtracting the fitness effect for the low-Fe^{2+} condition from that under the high-Fe^{2+} condition. A net fitness effect of $\geq \pm 1.0$ was considered significant, a threshold that has been found in our hands to be a good predictor of whether a specific mutation has a significant effect on fitness. To avoid statistical anomalies, genes with fewer than 1,000 mapped reads to the parent library were omitted from consideration in this study (see the "Curated fitness values" tab in Table S1).

TABLE 2 Bacterial strains and plasmids used in this study

Strain or plasmid	Description	Source or reference
Strains		
JG274	*S. oneidensis* MR-1, wild type	1
JG2989	JG274 Δ*feoE*	21
JG3354	JG274 Δ*rpoE*	This work
JG3355	JG274 Δ*clpPX*	This work
JG3486	JG274 Δ*clpP*	This work
JG3492	JG274 Δ*clpX*	This work
JG3552	JG274 Δ*smpB*	This work
JG3556	JG274 Δ*clpA*	This work
JG3560	JG274 Δ*smpB* Δ*clpP* Δ*clpA*	This work
JG3565	JG274 Δ*smpB* Δ*clpPX*	This work
JG3632	JG274 Δ*smpB* Δ*clpPX* Δ*clpA*	This work
JG168	JG274 with empty pBBR1MCS-2, Km^r	71
JG3488	JG3355 with empty pBBR1MCS-2, Km^r	This work
JG3549	JG3486 with empty pBBR1MCS-2, Km^r	This work
JG3495	JG3355 with pBBR1MCS-2::$clpPX_{MR-1}$	This work
JG3667	JG3355 with pBBR1MCS-2::$clpPX_{E.\ coli}$	This work
JG3668	JG3492 with pBBR1MCS-2::$clpX_{E.\ coli}$	This work
JG3570	JG3560 with pBBR1MCS-2::$clpP^{Tag}$	This work
JG3599	JG3560 with pBBR1MCS-2::$clpP^{Trap}$	This work
JG3600	JG3565 with pBBR1MCS-2::$clpP^{Trap}$	This work
JG3635	JG3632 with pBBR1MCS-2::$clpP^{Trap}$	This work
UQ950	*E. coli* DH5α λ(*pir*) cloning host; F^- Δ(*argF-lac*)*169* ϕ80d*lacZ58*(ΔM15) *glnV44*(AS) *rfbD1 gyrA96*(NalR) *recA1 endA1 spoT1 thi-1 hsdR17 deoR* λ*pir*$^+$	70
WM3064	*E. coli* conjugation strain; *thrB1004 pro thi rpsL hsdS lacZ*ΔM15 RP4–1360 Δ(*araBAD*)*567* Δ*dapA1341*::[*erm pir*(wild type)]	70
MG1655	*E. coli* K-12, wild type	Arkady Khodursky, University of Minnesota
JG3804	MG1655 Δ*clpP*	This study
JG3805	MG1655 Δ*clpX*	This study
Plasmids		
pSMV3	Deletion vector, Km^r *sacB*	79
pSMV3Δ*clpP*	pSMV3 with SO_1794 flanking sequences	This work
pSMV3Δ*clpX*	pSMV3 with SO_1795 flanking sequences	This work
pSMV3Δ*clpPX*	pSMV3 with SO_1794–5 flanking sequences	This work
pSMV3Δ*rpoE*	pSMV3 with SO_1342 flanking sequences	This work
pSMV3Δ*clpA*	pSMV3 with SO_2626 flanking sequences	This work
pSMV3Δ*smpB*	pSMV3 with SO_1473 flanking sequences	This work
pSMV3Δ$clpP_{EC}$	pSMV3 with b0437 flanking sequences	This work
pSMV3Δ$clpX_{EC}$	pSMV3 with b0438 flanking sequences	This work
pBBR1MCS-2	Broad-range cloning vector, Km^r	80
pBBR1MCS-2::$clpPX_{MR-1}$	SO_1794–5 (*clpPX*), 26 bp upstream, 8 bp downstream	This work
pBBR1MCS-2::$clpPX_{E.\ coli}$	b0437–8 (*clpPX*), 22 bp upstream, 28 bp downstream	This work
pBBR1MCS-2::$clpX_{E.\ coli}$	b0438 (*clpX*), 30 bp upstream, 28 bp downstream	This work
pBBR1MCS-2::$clpP^{Tag}$	SO_1794 (*clpP*) Δ2–9, downstream HIS_6-TEV-MYC_3	This work
pBBR1MCS-2::$clpP^{Trap}$	SO_1794 (*clpP*) Δ2–9, S106A, downstream HIS_6-TEV-MYC_3	This work

Plasmid and mutant construction. Table 3 lists the primers used for construction of deletion and expression plasmids. In-frame deletion of genes was performed via homologous recombination as described in Saltikov et al. (70). Briefly, 1-kb upstream and downstream fragments for each gene were fused via a restriction site and inserted into the multiple-cloning site of pSMV3, which has kanamycin resistance and *sacB* cassettes. Complementation plasmids were created by cloning *clpPX* from the *S. oneidensis* genome and *clpPX* and *clpX* from the *E. coli* MG1655 genome and inserted into the multiple-cloning site of the constitutive expression vector pBBR1MCS-2 via BamHI and SpeI restriction sites. Tagged genes for protein purification were ordered as gBlocks from Integrated DNA Technologies and ligated into the expression vector pBBR1MCS-2 via EcoRI and BamHI restriction sites. Tagged alleles of *clpP* were created without the propeptide sequence (missing amino acids 2 to 9), with a C-terminal affinity (His_6-TEV-Myc_3) tag codon optimized for *S. oneidensis*, and with or without a deactivating point mutation in the active site (S106A), creating $clpP^{Trap}$ and $clpP^{Tag}$, respectively. $clpP^{Tag}$ and $clpP^{Trap}$ sequences are listed in Table S2 in the supplemental material.

Growth curves. Overnight liquid LB cultures were grown from freshly isolated colonies. Cells were pelleted by centrifugation, washed once, and resuspended in either LB or SBM, depending on the culture medium to be used. Fe^{2+} cultures were supplemented with 0.8 mM $FeCl_2$ for SBM or either 2 or 2.5 mM $FeCl_2$ for LB. A higher Fe^{2+} concentration was needed for growth curves in LB than in SBM to visualize

TABLE 3 Primer sequences used for mutation and complementation in this work

Primer	Sequence	Restriction site
S. oneidensis		
rpoE deletion		
1342USF	GTACGGATCCCAATGCTTCGGTCAGCAG	BamHI
1342USR	GTACACTAGTCTCATCCGAGCCGACTTC	SpeI
1342DSF	GTACACTAGTGCCTTTGCTGGAAGAGTAAATTC	SpeI
1342DSR	GTACGAGCTCCACCCTGAATATGATTAGAGAGG	SacI
clpP deletion		
1794USF	GTACGGATCCGATGTGGACAGCATGATTG	BamHI
1794USR	GTACACTAGTGGCGAACTGCTAATCAAGTC	SpeI
1794DSF	GTACACTAGTGATTTTTACTTTCGACTGGGC	SpeI
1794DSR	GTACGAGCTCCTCAACTTGAGACAGGGTTTC	SacI
clpX deletion		
1795USF	GTACGGATCCCTCTATGGCTTCTGCTTACG	BamHI
1795USR	GTACACTAGTGCCCATTAATTACCTCATTTGC	SpeI
1795DSF	GTACACTAGTGGCGAGCAATAATTGTACAG	SpeI
1795DSR	GTACGAGCTCCAGACATCGGTGACATCATG	SacI
clpA deletion		
2626USF	GTACGAGCTCCGCTAAACAAGCTATTGATTG	SacI
2626USR	GTACGAATTCCAGATCTTTGTTCAGCATAAGC	EcoRI
2626DSF	GTACGAATTCGCTTAACGCCAAGCTAATTTAC	EcoRI
2626DSR	GCATACTAGTCTATTAGCCATAGGCTTTCG	SpeI
smpB deletion		
1473USF	GTACGAGCTCCTTCATCCTTGGCTTTATCAG	SacI
1473USR	GTACGAATTCGTTTTTCTTTACCATAGTGGC	EcoRI
1473DSF	GTACGAATTCGGATAATGAACAAACGATTGAAC	EcoRI
1473DSR	GTACACTAGTGCAATCTGTGCTTCTCTATG	SpeI
clpPX expression		
1794F	GTACGGATCCGCCATTTTTATTTAGGGAAATG	BamHI
1795R	GTACACTAGTCTGTACAATTATTGCTCGCC	SpeI
E. coli		
clpP deletion		
b0437USF	GTACACTAGTGAAGAATACCACGCAGAAAAC	SpeI
b0437USR	GTACGCGGCCGCCTGTATGACATTTCCGTCTCC	NotI
b0437DSF	GTACGCGGCCGCCATCGTAATTGATGCCAGAGG	NotI
b0437DSR	GTACGAGCTCCGGACTTCGCTTTTACCG	SacI
clpX deletion		
b0438USF	GTACGAGCTCCCGTACCCATAACACAGG	SacI
b0438USR	GTACGCGGCCGCGCCATCTTTGCGTTTATC	NotI
b0438DSF	GTACGCGGCCGCGCATCTGGTGAATAATTAACC	NotI
b0438DSR	GTACACTAGTGCTCGTTCAGATAGTACTCAC	SpeI
clpPX and *clpX* expression		
ECb0437F	GTACGGATCCCAATTTTATCCAGGAGACGG	BamHI
ECb0438F	GTACGGATCCGCACAAAGAACAAAGAAGAGG	BamHI
ECb0438R	GTACACTAGTGGTTAACTAATTGTATGGGAATGG	SpeI

the growth defects of mutants. Slightly different concentrations of $FeCl_2$ were required in different batches of media to achieve a toxic effect while allowing for cell growth. Growth was measured by taking the optical density at 600 nm (OD_{600}). Results are reported as the mean ± 1 standard deviation from three biological replicates. Growth curves were performed in triplicate at least twice; the results reported here are representative of each experiment.

ClpP trapping and protein purification. A previously described ClpP trapping protocol (25) was adapted for *S. oneidensis*. Briefly, the Δ*smpB* Δ*clpP* Δ*clpA*, and Δ*smpB* Δ*clpPX* mutants and the Δ*smpB* Δ*clpPX* Δ*clpA* mutant with pBBR1MCS-2::$clpP^{Trap}$ were grown anaerobically for 12 h in 1 liter anaerobic LB supplemented with 20 mM lactate and 40 mM fumarate; the Δ*smpB* Δ*clpP* Δ*clpA* mutant with pBBR1MCS-2::$clpP^{Trap}$ was also grown for 12 h in in 3 liters anaerobic LB supplemented with 20 mM lactate, 40 mM fumarate, and 1.1 mM $FeCl_2$. A 1.1 mM concentration of $FeCl_2$ was chosen because *clpP* mutant strains

are impaired but still able to grow at this concentration (data not shown). Cells were centrifuged 10 min at 5,000 rpm, resuspended in 40 ml Tris-buffered saline with 1 mM EDTA and 10 μM phenylmethylsulfonyl fluoride (pH 7.5), and centrifuged for 10 min at 5,000 rpm. Cell pellets were resuspended in 40 ml Tris-buffered saline and 10 μM phenylmethylsulfonyl fluoride (pH 8.0) and lysed by passing through a French press three times at 1,200 lb/in^2. The lysate was centrifuged for 20 min at 10,000 rpm. The lysate supernatant was incubated with 4 ml anti-c-Myc–agarose (25% slurry; Thermo Scientific) for 5 h on a rocker at 4°C. The resin was collected on a 10-ml column and washed with 10 ml Tris-buffered saline with 0.5% Tween 20. The resin was eluted with 4 ml 50 mM NaOH, which was concentrated to 100 μl in a SpeedVac (Thermo Scientific).

Protein analysis. Twenty micrograms of each protein elution was run into a Bio-Rad 8 to 16% Criterion precast polyacrylamide gel for 22 min at 25 mA. A single band for each sample containing total trapped protein was excised, digested in-gel with trypsin, and analyzed by liquid chromatography-tandem mass spectrometry (LC-MS/MS) on Thermo Orbitrap Velos and Orbitrap Fusion mass spectrometers. Detected peptides were mapped to *S. oneidensis* MR-1 protein and decoy (RefSeq *Shewanella* 70863) and common laboratory contaminant databases with Scaffold (Proteome Software, Inc.). Proteins with fewer than two spectra overall or more than one missed cleavage were excluded from analysis. The protein threshold was set at 99.0% minimum, a protein false-discovery rate (FDR) of 9%, a peptide threshold of 95.0% minimum, and a peptide FDR of 0.3%. The abundance of proteins trapped by ClpP^{Trap} for each sample was quantified by evaluating both exclusive spectrum counts and the percentage of total spectra for each protein. Complete Scaffold results are listed in Table S3. Protein cofactors were predicted using Uniprot (77) and the Conserved Domain Database (78).

SUPPLEMENTAL MATERIAL

Supplemental material for this article may be found at https://doi.org/10.1128/JB.00671-17.

SUPPLEMENTAL FILE 1, XLSX file, 3.1 MB.
SUPPLEMENTAL FILE 2, PDF file, 0.1 MB.
SUPPLEMENTAL FILE 3, XLSX file, 0.1 MB.

ACKNOWLEDGMENTS

We thank LeeAnn Higgins and Todd Markowski at the Center for Mass Spectrometry and Proteomics at the University of Minnesota for proteomics guidance and mass spectrometry analysis. We also thank Rebecca Maysonet for help with *E. coli* work.

This work was supported by the Office of Naval Research (N00014-13-1-0552 to J.A.G.). B.D.B. was supported in part by the University of Minnesota Biotechnology Training Grant Program through the National Institutes of Health. K.E.R. was supported by a MnDRIVE Seed Grant for Undergraduate Scholars.

REFERENCES

1. Myers CR, Nealson KH. 1988. Bacterial manganese reduction and growth with manganese oxide as the sole electron acceptor. Science 240:1319–1321. https://doi.org/10.1126/science.240.4857.1319.
2. Nealson KH, Myers CR, Wimpee BB. 1991. Isolation and identification of manganese-reducing bacteria and estimates of microbial Mn(IV)-reducing potential in the Black Sea. Deep Sea Res 38:S907–S920. https://doi.org/10.1016/S0198-0149(10)80016-0.
3. Brettar I, Höfle MG. 1993. Nitrous oxide producing heterotrophic bacteria from the water column of the central Baltic: abundance and molecular identification. Mar Ecol Prog Ser 94:253–265. https://doi.org/10.3354/meps094253.
4. Samuelsson MO. 1985. Dissimilatory nitrate reduction to nitrate, nitrous oxide, and ammonium by *Pseudomonas putrefaciens*. Appl Environ Microbiol 50:812–815.
5. Shirodkar S, Reed S, Romine Saffarini MD. 2011. The octahaem SirA catalyses dissimilatory sulfite reduction in *Shewanella oneidensis* MR-1. Environ Microbiol 13:108–115. https://doi.org/10.1111/j.1462-2920.2010.02313.x.
6. Kostka JE, Nealson KH. 1995. Dissolution and reduction of magnetite by bacteria. Environ Sci Technol 29:2535–2540. https://doi.org/10.1021/es00010a012.
7. Canfield DE. 1989. Reactive iron in marine sediments. Geochim Cosmochim Acta 53:619–632. https://doi.org/10.1016/0016-7037(89)90005-7.
8. Schwertmann U. 1991. Solubility and dissolution of iron oxides. Plant Soil 130:1–25. https://doi.org/10.1007/BF00011851.
9. O'Reilly SE, Watkins J, Furukawa Y. 2005. Secondary mineral formation associated with respiration of nontronite, NAu-1 by iron reducing bacteria. Geochem Trans 6:67–76. https://doi.org/10.1186/1467-4866-6-67.
10. Riordan JF. 1977. The role of metals in enzyme activity. Ann Clin Lab Sci 7:119–129.
11. Moore B, Hawkes JL. 1908. An investigation of the toxic actions of dilute solutions of the salts of certain heavy metals (viz.: copper, iron, nickel, cobalt, manganese, zinc, silver, and lead) upon the *Bacillus typhosus*, with a view to practical application in the purification of shell-fish. Biochem J 3:313–345. https://doi.org/10.1042/bj0030313.
12. Stohs SJ, Bagchi D. 1995. Oxidative mechanisms in the toxicity of metal ions. Free Radic Biol Med 18:321–336. https://doi.org/10.1016/0891-5849(94)00159-H.
13. Dunning JC, Ma Y, Marquis RE. 1998. Anaerobic killing of oral streptococci by reduced, transition metal cations. Appl Environ Microbiol 64:27–33.
14. Sutton HC. 1985. Efficiency of chelated iron compounds as catalysts for the Haber-Weiss reaction. J Free Radic Biol Med 1:195–202. https://doi.org/10.1016/0748-5514(85)90118-7.
15. Touati D, Jacques M, Tardat B, Bouchard L, Despied S. 1995. Lethal oxidative damage and mutagenesis are generated by iron in delta *fur* mutants of *Escherichia coli*: protective role of superoxide dismutase. J Bacteriol 177:2305–2314. https://doi.org/10.1128/jb.177.9.2305-2314.1995.
16. Berman T, Kaplan B, Chava S, Parparova R, Nishri A. 1993. Effects of iron and chelation on Lake Kinneret bacteria. Microb Ecol 26:1–8. https://doi.org/10.1007/BF00166024.
17. Kersters I, Verstraete W. 1996. Inactivation of *Aeromonas hydrophila* by

Fe(II)-related-radical generation in oxidizing groundwaters. Appl Environ Microbiol 62:3277–3283.
18. Hantke K. 1981. Regulation of ferric iron transport in *Escherichia coli* K12: isolation of a constitutive mutant. Mol Gen Genet 182:288–292. https://doi.org/10.1007/BF00269672.
19. Wan XF, Verberkmoes NC, McCue LA, Stanek D, Connelly H, Hauser LJ, Wu L, Liu X, Yan T, Leaphart A, Hettich RL, Zhou J, Thompson DK. 2004. Transcriptomic and proteomic characterization of the Fur modulon in the metal-reducing bacterium *Shewanella oneidensis*. J Bacteriol 186:8385–8400. https://doi.org/10.1128/JB.186.24.8385-8400.2004.
20. Yang Y, Harris DP, Luo F, Wu L, Parsons AB, Palumbo AV, Zhou J. 2008. Characterization of the *Shewanella oneidensis* Fur gene: roles in iron and acid tolerance response. BMC Genomics 9(Suppl 1):S11. https://doi.org/10.1186/1471-2164-9-S1-S11.
21. Bennett BD, Brutinel ED, Gralnick JA. 2015. A ferrous iron exporter mediates iron resistance in *Shewanella oneidensis* MR-1. Appl Environ Microbiol 81:7938–7944. https://doi.org/10.1128/AEM.02835-15.
22. Wojtkowiak D, Georgopoulos C, Zylicz M. 1993. Isolation and characterization of ClpX, a new ATP-dependent specificity component of the Clp protease of *Escherichia coli*. J Biol Chem 268:22609–22617.
23. Hwang BJ, Park WJ, Chung CH, Goldberg AL. 1987. *Escherichia coli* contains a soluble ATP-dependent protease (Ti) distinct from protease La. Proc Natl Acad Sci U S A 84:5550–5554. https://doi.org/10.1073/pnas.84.16.5550.
24. Katayama-Fujimura Y, Gottesman S, Maurizi MR. 1987. A multiple-component, ATP-dependent protease from *Escherichia coli*. J Biol Chem 262:4477–4485.
25. Flynn JM, Neher SB, Kim YI, Sauer RT, Baker TA. 2003. Proteomic discovery of cellular substrates of the ClpXP protease reveals five classes of ClpX-recognition signals. Mol Cell 11:671–683. https://doi.org/10.1016/S1097-2765(03)00060-1.
26. Gottesman S, Clark WP, Maurizi MR. 1990. The ATP-dependent Clp protease of *Escherichia coli*. Sequence of *clpA* and identification of a Clp-specific substrate J Biol Chem 265:7886–7893.
27. Chung CH, Goldberg AL. 1981. The product of the *lon* (*capR*) gene in *Escherichia coli* is the ATP-dependent protease, protease La. Proc Natl Acad Sci U S A 78:4931–4935. https://doi.org/10.1073/pnas.78.8.4931.
28. Charette MF, Henderson GW, Markovitz A. 1981. ATP hydrolysis-dependent protease activity of the *lon* (*capR*) protein of *Escherichia coli* K-12. Proc Natl Acad Sci U S A 78:4728–4732. https://doi.org/10.1073/pnas.78.8.4728.
29. Chuang SE, Burland V, Plunkett G, III, Daniels DL, Blattner FR. 1993. Sequence analysis of four new heat-shock genes constituting the *hslTS*/*ibpAB* and *hslVU* operons in *Escherichia coli*. Gene 134:1–6. https://doi.org/10.1016/0378-1119(93)90167-2.
30. Herman C, Ogura T, Tomoyasu T, Hiraga S, Akiyama Y, Ito K, Thomas R, D'Ari R, Bouloc P. 1993. Cell growth and a phage development controlled by the same essential *Escherichia coli gene*, *ftsH*/*hflB*. Proc Natl Acad Sci U S A 90:10861–10865. https://doi.org/10.1073/pnas.90.22.10861.
31. Schweder T, Lee KH, Lomovskaya O, Matin A. 1996. Regulation of *Escherichia coli* starvation sigma factor (σ^S) by ClpXP protease. J Bacteriol 178:470–476. https://doi.org/10.1128/jb.178.2.470-476.1996.
32. Neher SB, Villén J, Oakes EC, Bakalarski CE, Sauer RT, Gygi SP, Baker TA. 2006. Proteomic profiling of ClpXP substrates after DNA damage reveals extensive instability within SOS regulon. Mol Cell 22:193–204. https://doi.org/10.1016/j.molcel.2006.03.007.
33. Buczek MS, Cardenas Arevalo AL, Janakiraman A. 2016. ClpXP and ClpAP control the *Escherichia coli* division protein ZapC by proteolysis. Microbiology 162:909–920. https://doi.org/10.1099/mic.0.000278.
34. Flynn JM, Levchenko I, Sauer RT, Baker TA. 2004. Modulating substrate choice: the SspB adaptor delivers a regulator of the extracytoplasmic-stress response to the AAA+ protease ClpXP for degradation. Genes Dev 18:2292–2301. https://doi.org/10.1101/gad.1240104.
35. Gottesman S, Roche E, Zhou Y, Sauer RT. 1998. The ClpXP and ClpAP proteases degrade proteins with carboxy-terminal peptide tails added by the SsrA-tagging system. Genes Dev 12:1338–1347. https://doi.org/10.1101/gad.12.9.1338.
36. Baker TA, Sauer RT. 2012. ClpXP, an ATP-powered unfolding and protein-degradation machine. Biochim Biophys Acta 1823:15–28. https://doi.org/10.1016/j.bbamcr.2011.06.007.
37. Kammler M, Schön C, Hantke K. 1993. Characterization of the ferrous iron uptake system of *Escherichia coli*. J Bacteriol 175:6212–6219. https://doi.org/10.1128/jb.175.19.6212-6219.1993.
38. Chandu D, Nandi D. 2004. Comparative genomics and functional roles of the ATP-dependent proteases Lon and Clp during cytosolic protein degradation. Res Microbiol 155:710–719. https://doi.org/10.1016/j.resmic.2004.06.003.
39. Frees D, Savijoki K, Varmanen P, Ingmer H. 2007. Clp ATPases and ClpP proteolytic complexes regulate vital biological processes in low GC, Gram-positive bacteria. Mol Microbiol 63:1285–1295. https://doi.org/10.1111/j.1365-2958.2007.05598.x.
40. Voos W, Jaworek W, Wilkening A, Bruderek M. 2016. Protein quality control at the mitochondrion. Essays Biochem 60:213–225. https://doi.org/10.1042/EBC20160009.
41. Karzai AW, Susskind MM, Sauer RT. 1999. SmpB, a unique RNA-binding protein essential for the peptide-tagging activity of SsrA (tmRNA). EMBO J 18:3793–3799. https://doi.org/10.1093/emboj/18.13.3793.
42. Levchenko I, Seidel M, Sauer RT, Baker TA. 2000. A specificity-enhancing factor for the ClpXP degradation machine. Science 289:2354–2356. https://doi.org/10.1126/science.289.5488.2354.
43. Brutinel ED, Gralnick JA. 2012. Anomalies of the anaerobic tricarboxylic acid cycle in *Shewanella oneidensis* revealed by Tn-seq. Mol Microbiol 86:273–283. https://doi.org/10.1111/j.1365-2958.2012.08196.x.
44. Ades SE, Connolly LE, Alba BM, Gross CA. 1999. The *Escherichia coli* sigma(E)-dependent extracytoplasmic stress response is controlled by the regulated proteolysis of an anti-sigma factor. Genes Dev 13:2449–2461. https://doi.org/10.1101/gad.13.18.2449.
45. Saito A, Hizukuri Y, Matsuo E, Chiba S, Mori H, Nishimura O, Ito K, Akiyama Y. 2011. Post-liberation cleavage of signal peptides is catalyzed by the site-2 protease (S2P) in bacteria. Proc Natl Acad Sci U S A 108:13740–13745. https://doi.org/10.1073/pnas.1108376108.
46. De Las Peñas A, Connolly L, Gross CA. 1997. The σ^E-mediated response to extracytoplasmic stress in *Escherichia coli* is transduced by RseA and RseB, two negative regulators of σ^E. Mol Microbiol 24:373–385. https://doi.org/10.1046/j.1365-2958.1997.3611718.x.
47. Singh SK, Grimaud R, Hoskins JR, Wickner S, Maurizi MR. 2000. Unfolding and internalization of proteins by the ATP-dependent proteases ClpXP and ClpAP. Proc Natl Acad Sci U S A 97:8898–8903. https://doi.org/10.1073/pnas.97.16.8898.
48. Erbse A, Schmidt R, Bornemann T, Schneider-Mergener J, Mogk A, Zahn R, Dougan DA, Bukau B. 2006. ClpS is an essential component of the N-end rule pathway in *Escherichia coli*. Nature 439:753–756. https://doi.org/10.1038/nature04412.
49. De Las Peñas A, Connolly L, Gross CA. 1997. SigmaE is an essential sigma factor in *Escherichia coli*. J Bacteriol 179:6862–6864. https://doi.org/10.1128/jb.179.21.6862-6864.1997.
50. Xia W, Li H, Sze KH, Sun H. 2009. Structure of a nickel chaperone, HypA, from Helicobacter pylori reveals two distinct metal binding sites. J Am Chem Soc 131:10031–10040. https://doi.org/10.1021/ja900543y.
51. Konopka K. 1978. Differential effects of metal-binding agents on the uptake of iron from transferrin by isolated rat liver mitochondria. FEBS Lett 92:308–312. https://doi.org/10.1016/0014-5793(78)80776-5.
52. Floyd RA, Lewis CA. 1983. Hydroxyl free radical formation from hydrogen peroxide by ferrous iron-nucleotide complexes. Biochemistry 22:2645–2649. https://doi.org/10.1021/bi00280a008.
53. Yamashita MM, Wesson L, Eisenman G, Eisenberg D. 1990. Where metal ions bind in proteins. Proc Natl Acad Sci U S A 87:5648–5652. https://doi.org/10.1073/pnas.87.15.5648.
54. Irving H, Williams RJP. 1953. The stability of transition-metal complexes. J Chem Soc 1953:3192–3210. https://doi.org/10.1039/jr9530003192.
55. Leimkühler S, Wuebbens MM, Rajagopalan KV. 2011. The history of the discovery of the molybdenum cofactor and novel aspects of its biosynthesis in bacteria. Coord Chem Rev 255:1129–1144. https://doi.org/10.1016/j.ccr.2010.12.003.
56. Argüello JM, Raimunda D, Padilla-Benavides T. 2013. Mechanisms of copper homeostasis in bacteria. Front Cell Infect Microbiol 3:73. https://doi.org/10.3389/fcimb.2013.00073.
57. Ferreira GC, Franco R, Lloyd SG, Moura I, Moura JJG, Huynh BH. 1995. Structure and function of ferrochelatase. J Bioenerg Biomembr 27:221–229. https://doi.org/10.1007/BF02110037.
58. Brayman TG, Hausinger RP. 1996. Purification, characterization, and functional analysis of a truncated *Klebsiella aerogenes* UreE urease accessory protein lacking the histidine-rich carboxyl terminus. J Bacteriol 178:5410–5416. https://doi.org/10.1128/jb.178.18.5410-5416.1996.
59. Song HK, Mulrooney SB, Huber R, Hausinger RP. 2001. Crystal structure of *Klebsiella aerogenes* UreE, a nickel-binding metallochaperone for urease activation. J Biol Chem 276:49359–49364. https://doi.org/10.1074/jbc.M108619200.

60. Raux E, Thermes C, Heathcote P, Rambach A, Warren MJ. 1997. A role for *Salmonella typhimurium cbiK* in cobalamin (vitamin B12) and siroheme biosynthesis. J Bacteriol 179:3202–3212. https://doi.org/10.1128/jb.179.10.3202-3212.1997.
61. Raux E, Lanois A, Rambach A, Warren MJ, Thermes C. 1998. Cobalamin (vitamin B12) biosynthesis: functional characterization of the *Bacillus megaterium cbi* genes required to convert uroporphyrinogen III into cobyrinic acid a,c-diamide. Biochem J 335:167–173. https://doi.org/10.1042/bj3350167.
62. Tottey S, Waldron KJ, Firbank SJ, Reale B, Bessant C, Sato K, Cheek TR, Gray J, Banfield MJ, Dennison C, Robinson NJ. 2008. Protein-folding location can regulate manganese-binding versus copper- or zinc-binding. Nature 455:1138–1142. https://doi.org/10.1038/nature07340.
63. Hung H-C, Chang G-G. 2001. Differentiation of the slow-binding mechanism for magnesium ion activation and zinc ion inhibition of human placental alkaline phosphatase. Protein Sci 10:34–45. https://doi.org/10.1110/ps.35201.
64. Foster AW, Osman D, Robinson NJ. 2014. Metal preferences and metallation. J Biol Chem 289:28095–28103. https://doi.org/10.1074/jbc.R114.588145.
65. Hmiel SP, Snavely MD, Florer JB, Maguire ME, Miller CG. 1989. Magnesium transport in *Salmonella typhimurium*: genetic characterization and cloning of three magnesium transport loci. J Bacteriol 171:4742–4751. https://doi.org/10.1128/jb.171.9.4742-4751.1989.
66. Snavely MD, Florer JB, Miller CG, Maguire ME. 1989. Magnesium transport in *Salmonella typhimurium*: Mg^{2+} transport by the CorA, MgtA, and MgtB systems. J Bacteriol 171:4761–4766. https://doi.org/10.1128/jb.171.9.4761-4766.1989.
67. Niegowski D, Eshaghi S. 2007. The CorA family: structure and function revisited. Cell Mol Life Sci 64:2564–2574. https://doi.org/10.1007/s00018-007-7174-z.
68. Bird LJ, Coleman ML, Newman DK. 2013. Iron and copper act synergistically to delay anaerobic growth of bacteria. Appl Environ Microbiol 79:3619–3627. https://doi.org/10.1128/AEM.03944-12.
69. Chapman E, Farr GW, Usaite R, Furtak K, Fenton WA, Chaudhuri TK, Hondorp ER, Matthews RG, Wolf SG, Yates JR, Pypaert M, Horwich AL. 2006. Global aggregation of newly translated proteins in an Escherichia coli strain deficient of the chaperonin GroEL. Proc Natl Acad Sci U S A 103:15800–15805. https://doi.org/10.1073/pnas.0607534103.
70. Saltikov CW, Newman DK. 2003. Genetic identification of a respiratory arsenate reductase. Proc Natl Acad Sci U S A 100:10983–10988. https://doi.org/10.1073/pnas.1834303100.
71. Hau HH, Gilbert A, Coursolle D, Gralnick JA. 2008. Mechanism and consequences of anaerobic respiration of cobalt by *Shewanella oneidensis* strain MR-1. Appl Environ Microbiol 74:6880–6886. https://doi.org/10.1128/AEM.00840-08.
72. Balch WE, Fox GE, Magrum LJ, Woese CR, Wolfe RS. 1979. Methanogens: reevaluation of a unique biological group. Microbiol Rev 43:260–296.
73. Marsili E, Baron DB, Shikhare ID, Coursolle D, Gralnick JA, Bond DR. 2008. *Shewanella* secretes flavins that mediate extracellular electron transfer. Proc Natl Acad Sci U S A 105:3968–3973. https://doi.org/10.1073/pnas.0710525105.
74. Bouhenni R, Gehrke A, Saffarini D. 2005. Identification of genes involved in cytochrome c biogenesis in *Shewanella oneidensis*, using a modified mariner transposon. Appl Environ Microbiol 71:4935–4937. https://doi.org/10.1128/AEM.71.8.4935-4937.2005.
75. van Opijnen T, Bodi KL, Camilli A. 2009. Tn-seq: high-throughput parallel sequencing for fitness and genetic interaction studies in microorganisms. Nat Methods 6:767–772. https://doi.org/10.1038/nmeth.1377.
76. van Opijnen T, Camilli A. 2010. Genome-wide fitness and genetic interactions determined by Tn-Seq, a high-throughput massively parallel sequencing method for microorganisms. Curr Protoc Microbiol Chapter 1:Unit1E.3. https://doi.org/10.1002/9780471729259.mc01e03s19.
77. UniProt Consortium. 2015. UniProt: a hub for protein information. Nucleic Acids Res 43(Database issue):D204–D212. https://doi.org/10.1093/nar/gku989.
78. Marchler-Bauer A, Derbyshire MK, Gonzales NR, Lu S, Chitsaz F, Geer LY, Geer RC, He J, Gwadz M, Hurwitz DI, Lanczycki CJ, Lu F, Marchler GH, Song JS, Thanki N, Wang Z, Yamashita RA, Zhang D, Zheng C, Bryant SH. 2015. CDD: NCBI's conserved domain database. Nucleic Acids Res 43(Database issue):D222–D226. https://doi.org/10.1093/nar/gku1221.
79. Coursolle D, Gralnick JA. 2010. Modularity of the Mtr respiratory pathway of *Shewanella oneidensis* strain MR-1. Mol Microbiol 77:995–1008. https://doi.org/10.1111/j.1365-2958.2010.07266.x.
80. Kovach ME, Elzer PH, Hill DS, Robertson GT, Farris MA, Roop RM, Peterson KM. 1995. Four new derivatives of the broad-host-range cloning vector pBBR1MCS, carrying different antibiotic-resistance cassettes. Gene 166:175–176. https://doi.org/10.1016/0378-1119(95)00584-1.
81. Waldron KJ, Robinson NJ. 2009. How do bacterial cells ensure that metalloproteins get the correct metal? Nat Rev Microbiol 7:25–35. https://doi.org/10.1038/nrmicro2057.